Solution Dynamics of the Reversible Carbonyl–Phosphorus Ligand Exchange in $[(OC)_4\overline{Mo(\mu\text{-}PEt_2)_2Mo}(CO)_4]$: Kinetic Parameters as a Measure of the Relative Steric Hindrance of Phosphines and Phosphites *

Marino Basato
Centro di Studio sulla Stabilitá e Reattivitá dei Composti di Coordinazione, C.N.R., Istituto di Chimica Analitica, University of Padova, via Marzolo 1, 35100 Padova, Italy

Di-μ-diethylphosphido-bis(tetracarbonylmolybdenum) (*Mo–Mo*) undergoes reversible carbonyl substitution with phosphorus ligands in decalin, giving $[(OC)_4\overline{Mo(\mu\text{-}PEt_2)_2Mo}(CO)_3L]$ [L = $P(OEt)_3$, PMe_2Ph, PBu^n_3, $PMePh_2$, $PH(C_6H_{11})_2$, PPh_3, or $PPh_2(C_6H_{11})$]. Both the forward and reverse reactions occur by a dissociative mechanism involving the reactive intermediate $[(OC)_4\overline{Mo(\mu\text{-}PEt_2)_2Mo}(CO)_3]$, which has a co-ordinatively unsaturated six-co-ordinate molybdenum atom. The reactivity towards substitution depends on the relative rates of bimolecular attack of CO, k_{-1}, and of the phosphorus ligand, k_2, on this intermediate. Values of the competition ratio k_{-1}/k_2 range, at 100 °C, from 4.38 [L = $P(OEt)_3$] to 2.09×10^5 [L = $PPh_2(C_6H_{11})$], mainly as a consequence of a more favourable activation entropy for the smaller triethyl phosphite. The unexpected high sensitivity of the co-ordinatively unsaturated metal centre towards the steric hindrance of the incoming group is nicely demonstrated by plotting the differences in activation entropy $\Delta S_{-1}^{\ddagger} - \Delta S_2^{\ddagger}$ against Tolman's cone angle for the various phosphorus ligands. A good straight line is obtained, whose slope (4.6 J K^{-1} mol^{-1} $degree^{-1}$) can be assumed as the kinetic selectivity of the intermediate towards the size of the entering ligand. Activation parameters corresponding to the rate constants and competition ratios, together with equilibrium data, are reported.

Di-μ-dialkylphosphido-bis(tetracarbonylmetal) (*M–M*) (M = Cr, Mo, or W) complexes, as a consequence of the high stability of the MPMP ring, do not undergo fragmentation in the usual substitution or redox reactions.[1,2] Furthermore, the closeness of the metal centres (2.90—3.06 Å)[3] suggests an unusual reactivity for this class of compounds.[4] A previous study has shown that di-μ-diethylphosphido-bis(tetracarbonylmolybdenum) (*Mo–Mo*), (**1**), reacts with tri-n-butylphosphine through a dissociative mechanism involving the unsaturated intermediate $[(OC)_4\overline{Mo(\mu\text{-}PEt_2)_2Mo}(CO)_3]$, which exhibits a surprising kinetic discrimination towards the nature of the entering ligand.[5]

In view of this result, and the wide interest in phosphido-bridged binuclear metal complexes[6] and, in general, in the reactivity of polynuclear complexes,[7] I report here a kinetic and mechanistic study of the reversible carbonyl-substitution reaction of complex (**1**) with a series of phosphines and phosphites of variable size and electronic character, in decalin [equation (1), L = $P(OEt)_3$, PMe_2Ph, $PMePh_2$, $PH(C_6H_{11})_2$, PPh_3, or $PPh_2(C_6H_{11})$].

$$[(OC)_4\overline{Mo(\mu\text{-}PEt_2)_2Mo}(CO)_4] + L \rightleftharpoons [(OC)_4\overline{Mo(\mu\text{-}PEt_2)_2Mo}(CO)_3L] + CO \quad (1)$$

Experimental

Materials.—Decalin (Baker Analysed Reagent) was stored over molecular sieves. The phosphorus ligands were prepared by standard methods, distilled under reduced pressure (or recrystallised) before use, and kept under argon. Argon and carbon monoxide were high purity ($\geqslant$ 99.9%) SIO products. Certified Ar–CO mixtures were provided by SIAD, relative errors in their analysed contents always being less than 0.5%.

The complex $[(OC)_4\overline{Mo(\mu\text{-}PEt_2)_2Mo}(CO)_4]$, (**1**), was prepared as previously described.[5] The monosubstituted derivatives $[(OC)_4\overline{Mo(\mu\text{-}PEt_2)_2Mo}(CO)_3L]$, (**2**), were generally prepared *in situ* under kinetic conditions and identified on the basis of the close similarity of their i.r. spectra (Table 1) with those of the fully characterised PBu^n_3[5] and PPh_3 derivatives. The latter was prepared by reaction of complex (**1**) (0.3 g, 0.5 mmol) with PPh_3 (2.1 g, 8.0 mmol) in carefully deoxygenated decalin (20 cm^3) at 100 °C under Ar. After 6 h, the solvent was removed under reduced pressure and the residue, dissolved in n-hexane, was chromatographed on an alumina column, with n-hexane as eluant. Two orange fractions were obtained; the second one containing $[(OC)_4\overline{Mo(\mu\text{-}PEt_2)_2Mo}(CO)_3(PPh_3)]$, which was crystallised from n-hexane as bright orange crystals, yield 40% (Found: C, 47.85; H, 4.15. Calc. for $C_{33}H_{35}Mo_2O_7P_3$: C, 47.85; H, 4.25%).

Procedures.—Solutions of the solid phosphines were prepared by weight or by addition with a microsyringe of a known volume of the liquid ones to the solvent. In all cases they were carefully deoxygenated by three freeze–pump–thaw cycles and transferred under the appropriate gas (Ar, CO, or CO–Ar mixtures) to the reaction vessel containing known amounts of the solid complex. Kinetic runs were generally carried out as previously described using an i.r. analysis of the reacting mixture. For reactions at higher than atmospheric pressure only, the starting solution was transferred, through stainless-steel tubing, to a small autoclave equipped with a microvalve from which at suitable times samples were removed for i.r. analysis on a Perkin-Elmer 457 spectrophotometer. Sodium chloride cells (1.0 mm) were used in the measurements, the reference cell being filled with a solution of the appropriate ligand. The pressure in the reaction vessel was controlled with a manometer and concentrations of carbon monoxide were calculated as previously stated.[8]

---

* *Non-S.I. unit employed:* atm = 101 325 Pa.

Table 1. I.r. spectra of $[(OC)_4M\overline{o(\mu\text{-}PEt_2)_2M}o(CO)_3L]$ [L = $P(OEt)_3$, PMe_2Ph, $PBu^n{}_3$, $PMePh_2$, $PH(C_6H_{11})_2$, PPh_3, or $PPh_2(C_6H_{11})$] complexes in the CO stretching region (cm^{-1}, decalin)

$P(OEt)_3$	2 040m	1 996m-s	1 948m (sh)	1 940vs	1 927m	1 891w
PMe_2Ph	2 039m	1 990m-s	1 946 (sh)	1 936vs	1 921m-w	1 884w
$PBu^n{}_3$	2 039m	1 990m-s	1 946 (sh)	1 936vs	1 921m	1 883m
$PMePh_2$	2 039m	1 994m-s	1 947 (sh)	1 938vs	1 921 (sh)	1 883w
$PH(C_6H_{11})_2$	2 040m	1 991m	1 948 (sh)	1 936vs	1 928 (sh)	1 880m
PPh_3	2 040m	1 995m	1 947 (sh)	1 939vs	1 927 (sh)	1 887w
$PPh_2(C_6H_{11})$	2 039m	1 997m	1 947 (sh)	1 938vs	1 919w	1 885w

Results

The general behaviour is very similar to that observed in the reaction of complex (**1**) with $PBu^n{}_3$. The reaction, as a rule, gives in two distinct stages the mono- and di-substituted complexes $[(OC)_4M\overline{o(\mu\text{-}PEt_2)_2M}o(CO)_3L]$ and $[L(OC)_3M\overline{o(\mu\text{-}PEt_2)_2M}o(CO)_3L]$; however, with the bulkier $PH(C_6H_{11})_2$, $PPh_2(C_6H_{11})$, and PPh_3 only monosubstitution occurs under CO. The two stages proceed under convenient experimental conditions at rather different rates, so that the study could easily be limited to the forward and reverse reaction of the first substitution.

Kinetic data were generally obtained under pseudo-first-order conditions using an excess of phosphorus ligand, $[L]/[(\mathbf{1})] \geqslant 20$, and, in the runs under CO, at a constant CO pressure. The rate of disappearance of complex (**1**) was determined by plotting $\lg(A_t - A_\infty)$ *vs.* time [A = absorbance of the peak of (**1**) at 2 027 cm^{-1}]. The observed rate constants $k_{obs.}$ then represent for substitution reactions going to completion the observed rate of the forward reaction k_f. In those reactions under CO, where an equilibrium between complexes (**1**) and (**2**) was reached, $A_\infty = A_e$ (absorbance at equilibrium) and the slope of the logarithmic plot gives the sum of the observed rate constants of the forward and reverse reactions $k_{obs.} = k_f + k_r$.[9] In this case the two terms were separated by introducing the spectrophotometrically determined concentration ratios, at equilibrium, of complexes (**1**) and (**2**). In all cases the semilogarithmic plots are linear to over three half-lives.

As a rule, the experimental conditions were chosen with the purpose of determining the effect of the entering phosphorus ligand on the rate of CO substitution. This choice led to some inaccuracy in the determination of k_r and K_c in the equilibration reactions as a consequence of a $[(\mathbf{2})]_e/[(\mathbf{1})]_e$ ratio much greater than unity. Despite these experimental limitations, there is overall a good consistency of the kinetic and equilibrium data starting from either (**1**) or (**2**), and at various CO pressures. Table 2 gives the experimental conditions employed together with the kinetic and equilibrium {from the $[(\mathbf{2})]_e/[(\mathbf{1})]_e$ ratio} data obtained.

The data in Table 2 indicate that: (*i*) k_f under Ar is constant, independent of the nature and concentration of the entering ligand; (*ii*) k_f under CO depends on the nature and concentration of the entering ligand, and on the carbon monoxide pressure; (*iii*) k_r is a constant for a given monosubstituted complex.

With L = $P(OEt)_3$ or PMe_2Ph quantitative formation of complex (**2**) occurred, both under Ar and 1 atm CO. The observed rate constants under CO increase with increasing phosphine concentration, reaching a limiting value corresponding to the rate observed under Ar. The forward reaction obeys the rate equation $k_f = a/\{1 + (b[CO]/[L])\}$, where a is equal to the limiting rate under Ar and b is a rate parameter which differs for the two ligands. The reverse reaction was studied by treating solutions of complex (**2**), prepared *in situ*, with CO at moderate pressure, *ca.* 12.5—18.0 atm, in the presence of low phosphine concentrations (3.9—11.6) × 10^{-3} mol dm^{-3}. Under these conditions an equilibrium mixture of complexes (**1**) and (**2**) was obtained. The reaction was monitored by following the change in absorbance of the peaks at 2 040 cm^{-1} [L = $P(OEt)_3$] or 2 039 cm^{-1} (L = PMe_2Ph) and/or 2 027 cm^{-1} (**1**).

With L = $PMePh_2$ under 1 atm CO pressure the reaction proceeded to an equilibrium mixture of complexes (**1**) and (**2**) and k_f obeys to the same rate equation for L = $P(OEt)_3$ and PMe_2Ph, which implies the same limiting rate.

With L = $PH(C_6H_{11})_2$, PPh_3, and $PPh_2(C_6H_{11})$ the reaction under carbon monoxide reached a substitution equilibrium, which is particularly unfavourable for the larger PPh_3 and $PPh_2(C_6H_{11})$ ligands. In these cases the values of k_f are much lower than the limiting rate under Ar observed for the previous ligands and are linearly dependent on the phosphine-to-carbon monoxide concentration ratio, according to $k_f = d[L]/[CO]$, d being different for the various ligands. Runs under Ar gave curved semilogarithmic plots as a consequence of the competing effect of CO released during the substitution reaction.

Discussion

The kinetic data are consistent for all the investigated phosphorus ligands with a reversible carbon monoxide substitution occurring through a dissociative mechanism [reactions (2) and (3); L = $P(OEt)_3$, PMe_2Ph, $PBu^n{}_3$,[5] $PMePh_2$, $PH(C_6H_{11})_2$, PPh_3, or $PPh_2(C_6H_{11})$]. If we apply the steady-state treatment

$$[(OC)_4M\overline{o(\mu\text{-}PEt_2)_2M}o(CO)_4] \underset{k_{-1}}{\overset{k_1}{\rightleftharpoons}} [(OC)_4M\overline{o(\mu\text{-}PEt_2)_2M}o(CO)_3] + CO \quad (2)$$

$$[(OC)_4M\overline{o(\mu\text{-}PEt_2)_2M}o(CO)_3] + L \underset{k_{-2}}{\overset{k_2}{\rightleftharpoons}} [(OC)_4M\overline{o(\mu\text{-}PEt_2)_2M}o(CO)_3L] \quad (3)$$

$$k_{obs.} = k_f + k_r = \frac{k_1}{1 + (k_{-1}[CO]/k_2[L])} + \frac{k_{-2}}{1 + (k_2[L]/k_{-1}[CO])} \quad (4)$$

to the reactive intermediate $[(OC)_4M\overline{o(\mu\text{-}PEt_2)_2M}o(CO)_3]$, when [L] and [CO] are constant and $[(\mathbf{1})] + [(\mathbf{2})] = [(\mathbf{1})]_0$ {or $[(\mathbf{2})]_0$}, the integrated rate equation is (4), where the two terms represent respectively the observed rate constants of the forward and reverse reactions. This is shown to be consistent with the experimental results as follows.

Equation (4) applied to the forward reaction coincides with that experimentally found with L = $P(OEt)_3$, PMe_2Ph, and $PMePh_2$, where $a = k_1$, the limiting rate of carbon monoxide dissociation, and $b = k_{-1}/k_2$, the competition ratio between the rates of attack of CO and L on the co-ordinatively unsaturated intermediate. The value of k_1 is of course independent of the type of entering ligand and can simply be determined from the

Table 2. Rate and equilibrium data for the reaction $[(OC)_4\overline{Mo(\mu\text{-}PEt_2)_2Mo}(CO)_4] + L \rightleftharpoons [(OC)_4\overline{Mo(\mu\text{-}PEt_2)_2Mo}(CO)_3L] + CO$ in decalin. [Complex][a] = $2 \times 10^{-4} - 1 \times 10^{-3}$ mol dm^{-3}

L	θ_c/°C	10^3[L]/mol dm^{-3}	y_{CO}[b]	10^3[CO]/mol dm^{-3}	$10^5(k_f + k_r)$/s^{-1}	$[(\mathbf{2})]_e/[(\mathbf{1})]_e$	10^5k_f/s^{-1}	10^5k_r/s^{-1}	K_c
$P(OEt)_3$	60.0	11.1	1.00	6.2			2.36		
		16.7	1.00	6.2			2.93		
		39.0	1.00	6.2			5.14		
		216	0.00	0.00			8.01		
		216	1.00	6.2			7.90		
	80.0	10.9	0.00	0.00			130		
		10.9	1.00	6.0			37.3		
		17.5	1.00	6.0			55.0		
		55.5	1.00	6.0			96.1		
		211	0.00	0.00			144		
		211	1.00	6.0			132		
	100.0	5.78	1.00[c]	*ca.* 70	96.1	2.80	70.8	25.3[d]	*ca.* 34
		11.6	1.00[c]	*ca.* 70	167	7.36	147	20.0[d]	*ca.* 44
PMe_2Ph	60.0	5.42	1.00	6.2			1.93		
		8.10	1.00	6.2			2.82		
		15.5	1.00	6.2			4.12		
		40.4	0.00	0.00			7.55		
		137	0.00	0.00			7.79		
		137	1.00	6.20			7.62		
	80.0	5.28	1.00	6.0			21.0		
		5.34	1.00	6.0			22.6		
		7.94	1.00	6.0			32.7		
		15.3	1.00	6.0			42.0		
		39.6	0.00	0.00			129		
		39.6	1.00	6.0			100		
		135	0.00	0.00			136		
	100.0	3.91	1.00[e]	*ca.* 100	34.0	2.30	23.7	10.3[d]	*ca.* 59
		6.51	1.00[c]	*ca.* 70	92.4	4.70	76.2	16.2[d]	*ca.* 51
$PMePh_2$	80.0	24.7	1.00	6.0	6.60	4.70	5.44	1.16	1.14
		50.1	1.00	6.0	12.2	7.03	10.7	1.52	0.84
		74.9	1.00	6.0	15.0	12.3	13.9	1.13	0.98
		99.5	1.00	6.0	23.0	17.8	21.8	1.22	1.07
	100.0	24.3	1.00	5.7	38.5	5.34	32.4	6.07	1.25
		49.3	1.00	5.7	71.1	12.9	66.0	5.12	1.49
		73.5	1.00	5.7	101	18.4	95.8	5.21	1.43
$PH(C_6H_{11})_2$	80.0	11.9	1.00	6.0	2.63	0.92	1.26	1.37	0.46
		44.8	1.00	6.0	6.79	7.22	5.96	0.83	0.97
		77.9	1.00	6.0	11.0	*ca.* 21	10.5	*ca.* 0.5	
		109	1.00	6.0	14.4	*ca.* 40	14.1	*ca.* 0.3	
	100.0	11.7	1.00	5.7	13.8	1.42	8.10	5.70	0.69
		22.1	1.00	5.7	19.2	2.31	13.4	5.80	0.60
		43.9	1.00	5.7	35.0	5.57	29.7	5.33	0.72
		87.0	1.00	5.7	73.7	14.6	69.0	4.72	0.96
	120.0	11.3	1.00	5.2	77.0	1.20	42.0	35.0	0.55
		11.7	1.00	5.2	77.2	1.36	44.5	32.7	0.60
		21.7	1.00	5.2	123	4.00	98.4	24.6	0.96
PPh_3	90.0	<0.27	0.096	0.56				7.16[d,f]	
		<0.41	1.00	5.9				6.93[d,f]	
		<9.43	0.096	0.56				6.90[d,f]	
		282	0.096	0.56	15.2	1.81	9.79	5.41	3.59×10^{-3}
		409	0.096	0.56	20.2	2.83	14.9	5.27	3.87×10^{-3}
		537	0.096	0.56	26.2	4.28	21.2	4.96	4.46×10^{-3}
		574	0.251	1.47	14.2	1.85	9.22	4.98	4.74×10^{-3}
		581	0.096	0.56	25.7	4.00	20.6	5.14	3.86×10^{-3}
	100.0	<0.40	1.00	5.7				16.6[d,f]	
		<0.60	0.096	0.54				16.5[d,f]	
		106	0.096	0.54	20.0	0.67	8.02	12.0	3.41×10^{-3}
		266	0.096	0.54	30.4	1.71	19.2	11.2	3.47×10^{-3}
		266	0.096	0.54	33.5	1.67	21.0	12.5	3.39×10^{-3}
		392	0.096	0.54	46.2	2.28	32.1	14.1	3.14×10^{-3}
		534	0.096	0.54	56.8	3.55	44.3	12.5	3.59×10^{-3}
		534	0.498	2.8	23.6	0.65	9.30	14.3	3.41×10^{-3}
		570	0.251	1.42	35.3	1.58	21.6	13.7	3.94×10^{-3}
	110.0	<0.37	1.00	5.5				37.6[d,f]	
		<0.58	0.096	0.52				37.3[d,f]	
		91.5	0.096	0.52	51.0	0.88	23.9	27.1	5.00×10^{-3}
		183	0.096	0.52	57.7	1.43	34.0	23.7	4.06×10^{-3}

Table 2 (*continued*)

L	θ_c / °C	10^3[L] / mol dm^{-3}	y_{CO}[b]	10^3[CO] / mol dm^{-3}	$10^5(k_f + k_r)$ / s^{-1}	$[(\mathbf{2})]_e$ / $[(\mathbf{1})]_e$	10^5k_f / s^{-1}	10^5k_r / s^{-1}	K_c
PPh_3		211	0.251	1.37	55.0	0.53	19.1	35.9	3.44×10^{-3}
		278	0.096	0.52	87.8	2.00	58.5	29.3	3.74×10^{-3}
		353	0.096	0.52	116	3.30	89.0	27.0	4.86×10^{-3}
		530	0.096	0.52	169	3.57	132	37.0	3.50×10^{-3}
		563	0.251	1.37	102	1.65	63.5	38.5	4.02×10^{-3}
$PPh_2(C_6H_{11})$	100.0	221	0.096	0.54	5.11	2.04	3.43	1.68	4.98×10^{-3}
		310	0.096	0.54	5.45	3.23	4.16	1.29	5.63×10^{-3}
		551	0.096	0.54	7.22	7.20	6.34	0.88	7.06×10^{-3}
		654	0.096	0.54	10.1	6.03	8.66	1.44	4.98×10^{-3}

[a] Starting from $[(OC)_4\overline{Mo(\mu\text{-}PEt_2)_2Mo}(CO)_4]$ or $[(OC)_4\overline{Mo(\mu\text{-}PEt_2)_2Mo}(CO)_3L]$. [b] Mole fraction of carbon monoxide in the CO–Ar mixture. Total pressure in the reaction vessel, including solvent vapour pressure, 1.1 atm. [c] p_{CO} = *ca.* 12.5 atm. [d] Starting from $[(OC)_4\overline{Mo(\mu\text{-}PEt_2)_2Mo}(CO)_3L]$, all other from $[(OC)_4\overline{Mo(\mu\text{-}PEt_2)_2Mo}(CO)_4]$. [e] p_{CO} = *ca.* 18 atm. [f] More accurate values used for the computation of k_r (see text).

Table 3. Rate and equilibrium constants[a] for the reaction $[(OC)_4\overline{Mo(\mu\text{-}PEt_2)_2Mo}(CO)_4] + L \rightleftharpoons [(OC)_4\overline{Mo(\mu\text{-}PEt_2)_2Mo}(CO)_3L] + CO$ in decalin

L	θ_c/°C	$10^5k_1{}^b$/s^{-1}	$10^6(k_1k_2/k_{-1})^b$/s^{-1}	$(k_{-1}/k_2)^b$	$10^5k_{-2}{}^c$/s^{-1}	K_c
$P(OEt)_3$	60.0	9.20(1.08)	17.2(2.0)	5.34(1.25)		
	80.0	153(11)	281(21)	5.44(0.78)		
	100.0				22	*ca.* 40
PMe_2Ph	60.0	7.67[d]	30.2(3.3)	2.88(0.65)		
	80.0	132[d]	272(44)	7.42(4.88)		
	100.0				12	*ca.* 55
$PMePh_2$	80.0	*ca.* 400	13.1(3.2)		1.23	0.98
	100.0	*ca.* 3 000	77.3(10.0)		5.40	1.37
$PH(C_6H_{11})_2$	80.0		7.40(0.71)[e]		0.97	5.58
	100.0		38.7(3.4)[e]		5.32	7.02
	120.0		206(27)[e]		29.3	6.35
PPh_3	90.0		0.209(0.011)[e]		6.99	4.02×10^{-3}
	100.0		0.440(0.022)[e]		16.5	3.45×10^{-3}
	110.0		1.21(0.09)[e]		37.4	3.94×10^{-3}
$PPh_2(C_6H_{11})$	100.0		0.071(0.007)[e]		1.17(0.28)	5.45×10^{-3}

[a] Uncertainties in parentheses are standard deviations (see text). [b] From the rate equation $1/k_f = (1/k_1) + (k_{-1}[CO]/k_1k_2[L])$; $\sigma(k_f)$ = 6.2—20%. [c] From the rate equation $k_r = k_{-2}$. [d] From the rate equation $k_f = k_1$. [e] From the rate equation $k_f[CO]/[L] = k_1k_2/k_{-1}$; $\sigma(k_f)$ = 11—23%.

rate of CO substitution under Ar. The same parameter together with the k_{-1}/k_2 values can be derived on rearrangement of the first term of equation (4) to $1/k_f = (1/k_1) + (k_{-1}[CO]/k_1k_2[L])$. This equation predicts linear plots of $1/k_f$ against $1/[L]$, at constant [CO], from which the values of k_1 and k_{-1}/k_2 can be derived. Consistent k_1 values were obtained from the reactions under Ar and under CO.

Equation (4) is also consistent with the substitution rate found with L = $PH(C_6H_{11})_2$, PPh_3, and $PPh_2(C_6H_{11})$, if it is assumed that here $k_{-1}[CO]/k_2[L] \gg 1$ so that the first term reduces to $k_f = k_1k_2[L]/k_{-1}[CO]$, where $d = k_1k_2/k_{-1}$. In this case the competition ratio k_{-1}/k_2 can be derived by introducing the value of the rate of CO dissociation, k_1, determined experimentally with the other entering phosphorus ligands.

Finally, it can easily be shown from the obtained k_{-1}/k_2 values that, under the experimental conditions employed to study the reverse reaction, $k_2[L]/k_{-1}[CO] \ll 1$, so that the second term of equation (4) reduces to $k_r = k_{-2}$, in agreement with the experimental behaviour.

All the reported rate and equilibrium constants were obtained by a least-squares analysis of the data and are collected in Table 3. The tabulated uncertainties are standard deviations corrected for the number of degrees of freedom, so that estimates of 95% confidence limits can be made by doubling the uncertainties. For a particular set of data, each $k_{obs.}$ (or K_c) value was weighted assuming the same percentage standard deviation at a given temperature. This procedure gave unrealistically high uncertainties for small sets of data, so that in most cases all pertinent kinetic (or equilibrium) data were pooled assuming the same percentage standard deviation at all the temperatures. For L = $P(OEt)_3$, PMe_2Ph, $PBu^n{}_3$,[5] and $PMePh_2$ the standard deviation of the ratio k_{-1}/k_2 takes into account the covariance of the parameters $1/k_1$ and k_{-1}/k_1k_2 obtained from the rate equation $1/k_f = (1/k_1) + (k_{-1}[CO]/k_1k_2[L])$. The fairly large uncertainty in the value of the intercept $1/k_1$ gives high standard deviations for k_{-1}/k_2 and the related activation parameters. The latter (Table 4) were, as a consequence, better calculated by combining the average $\Delta H_1^‡$ and $\Delta S_1^‡$ values for all investigated ligands with those relative to the individual k_1k_2/k_{-1} rate parameters. The resulting values for the activation parameters ($\Delta H_{-1}^‡ - \Delta H_2^‡$) and ($\Delta S_{-1}^‡ - \Delta S_2^‡$) and their standard deviations are, for the ligands listed above, slightly approximated.

For sake of clarity, Table 4 reports only selected kinetic and activation parameters. The omitted activation parameters for k_1 and k_1k_2/k_{-1} are irrelevant to the discussion and can easily be calculated from the specific rate constants in Table 3. For example, the average values $\Delta H_1^‡$ = 138(2) kJ mol^{-1} and

Table 4. Selected kinetic and activation parameters,[a] at 100 °C, for the reaction $[(OC)_4Mo(\mu\text{-}PEt_2)_2Mo(CO)_4] + L \rightleftharpoons [(OC)_4Mo(\mu\text{-}PEt_2)_2Mo(CO)_3L] + CO$ in decalin

	L						
	$P(OEt)_3$	PMe_2Ph	$PBu^n{}_3$[b]	$PMePh_2$	$PH(C_6H_{11})_2$	PPh_3	$PPh_2(C_6H_{11})$
(k_{-1}/k_2)[c]	4.38	8.27	84.5	178	351	3.28×10^4	2.09×10^5[d]
$(\Delta H_{-1}^‡ - \Delta H_2^‡)$/kJ mol^{-1}	4(6)	33(9)	34(4)	44(14)	46(4)	42(5)	—
$(\Delta S_{-1}^‡ - \Delta S_2^‡)$/J K^{-1} mol^{-1}	23(19)	106(27)	128(13)	161(37)	172(13)	199(14)	—
k_{-2}/s^{-1}	2.2×10^{-4}	1.2×10^{-4}	7.95×10^{-6}	5.40×10^{-5}	5.32×10^{-5}	1.65×10^{-4}	1.17×10^{-5}
$\Delta H_{-2}^‡$/kJ mol^{-1}	—	—	133(5)	78(7)	94(6)	94(1)	—
$\Delta S_{-2}^‡$/J K^{-1} mol^{-1}	—	—	12(12)	−120(20)	−75(17)	−67(2)	—

[a] See text; $\Delta H_1^‡ = 138(2)$ kJ mol^{-1}, $\Delta S_1^‡ = 88(6)$ J K^{-1} mol^{-1}, k_1 (extrapolated to 100 °C) = 1.48×10^{-2} s^{-1}. [b] From data in ref. 5. [c] From the activation parameters. [d] From the rate constant ratio k_1k_2/k_{-1}, by introducing the extrapolated k_1 value.

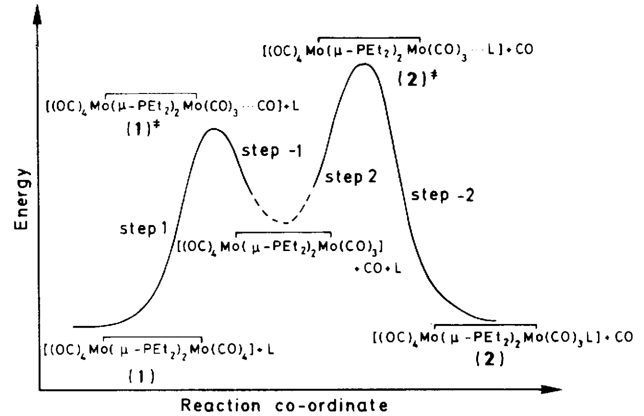

Figure 1. Plot of energy levels *versus* reaction co-ordinate for a typical reaction $[(OC)_4Mo(\mu\text{-}PEt_2)_2Mo(CO)_4] + L \rightleftharpoons [(OC)_4Mo(\mu\text{-}PEt_2)_2Mo(CO)_3L] + CO$

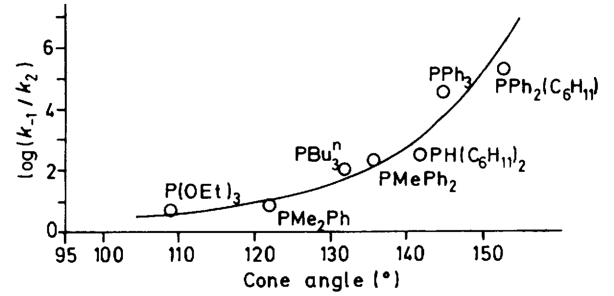

Figure 2. Plot of log (k_{-1}/k_2), at 100 °C, *versus* phosphorus ligand cone angle for the reaction $[(OC)_4Mo(\mu\text{-}PEt_2)_2Mo(CO)_4] + L \rightleftharpoons [(OC)_4Mo(\mu\text{-}PEt_2)_2Mo(CO)_3L] + CO$ in decalin. Values of ligand cone angle (°) from ref. 16: $P(OEt)_3$, 109; PMe_2Ph, 122; $PBu^n{}_3$, 132; $PMePh_2$, 136; PPh_3, 145; $PH(C_6H_{11})_2$, 142; $PPh_2(C_6H_{11})$, 153. The last two values were calculated by assuming approximate group additivity for cone angles, so that, for example, $\theta[PH(C_6H_{11})_2] = \frac{1}{3}\theta(PH_3) + \frac{2}{3}\theta[P(C_6H_{11})_3]$

$\Delta S_1^‡ = 88(6)$ J K^{-1} mol^{-1} are obtained as a weighted mean of the kinetic data for the phosphorus ligands employed in this and a previous[5] study.

The type of information which can be obtained from these parameters is better shown in Figure 1. We may determine the energy changes in step 1 and step −2, as well that in the overall substitution reaction (1) whereas those of steps −1 and 2 can be evaluated only as a difference between them.

Step 1.—This simply represents the conversion of the starting into the activated complex $(\mathbf{1})^‡$. The values of the activation parameters $\Delta H_1^‡ = 138(2)$ kJ mol^{-1} and $\Delta S_1^‡ = 88(6)$ J K^{-1} mol^{-1} are fully consistent with a CO-dissociative mechanism, in which extended bond breaking occurs, and are comparable with those previously reported for the CO-dissociative paths in substitution reactions of $[(OC)_4Cr(\mu\text{-}PEt_2)_2Cr(CO)_4]$, $[(OC)_4W(\mu\text{-}PEt_2)_2W(CO)_4]$,[10] $[L(OC)_2Co(\mu\text{-}C_2Ph_2)Co(CO)_3]$ (L = CO or $PBu^n{}_3$),[11] $[L(OC)_3Co(\mu\text{-}GePh_2)Co(CO)_4]$ (L = CO or PPh_3),[12] $[(Ph_3P)(OC)_2Fe(\mu\text{-}SPh)_2Fe(CO)_3]$,[13] and $[(OC)_3Fe(\mu\text{-}PPh_2)_2Fe(CO)_3]$.[14]

Steps −1 *and* 2.—Step −1 represents the recombination of the co-ordinatively unsaturated intermediate with CO to give the activated complex $(\mathbf{1})^‡$, whereas step 2 represents the attack of the entering phosphorus ligand on the same intermediate to give $(\mathbf{2})^‡$. The energy difference between steps −1 and 2 is a measure of how the intermediate discriminates between attack by CO and L; as step 2 is dependent on changes in the ligand, this difference is also a measure of how the intermediate discriminates between the various phosphines and phosphites. If one looks at the real nature of these steps, they simply represent the addition of the nucleophile CO or L to the electrophilic metal centre, so that the values of the competition ratio k_{-1}/k_2 can be assumed as a measure of the relative nucleophilicity of CO and the various phosphorus ligands towards the intermediate

The values of k_{-1}/k_2, at 100 °C, range from 4.38 $[P(OEt)_3]$ to 2.09×10^5 $[PPh_2(C_6H_{11})]$. A competition ratio of 2.09×10^5 for bimolecular attack on a co-ordinatively unsaturated complex is high compared with those previously found in other binuclear complexes of cobalt and iron,[11,13] and for bimolecular attack on mononuclear complexes;[15] in all these cases ratios of *ca.* 1 were found. Nevertheless it was expected on the basis of the previous observation that introduction of a $PBu^n{}_3$ molecule in complex (**1**) would make successive attack at the adjacent metal much more difficult. This was mainly explained in terms of an increased steric hindrance at the metal.[5] The prevalence of steric effects is confirmed in this study. Figure 2 shows the dependence of $\lg(k_{-1}/k_2)$ upon Tolman's cone angle.[16] A curve is obtained and the competition ratio k_{-1}/k_2 strongly changes in favour of CO attack as the phosphine (or phosphite) size increases.

A better insight into the intimate mechanism of these two steps can be gained by considering the nature of the intermediates $(\mathbf{1})^‡$ and $(\mathbf{2})^‡$ as can be inferred from the activation parameters for the four relevant steps 1, −1, 2, and −2.

Extensive Mo–CO bond breaking in (1)‡ justifies, as discussed above, the observed activation parameters for the CO-dissociative step 1; it can be anticipated here (see later) that the slightly positive or negative activation entropy values for the phosphorus ligand-dissociation step -2 are consistent with a very crowded intermediate (2)‡.

From the principle of microscopic reversibility, these conclusions must also hold for steps -1 and 2. Inspection of their activation parameters shows that the higher activation enthalpy for CO attack ($\Delta H_{-1}^\ddagger > \Delta H_2^\ddagger$) is dominated by a much more positive (or less negative) activation entropy. The values of $\Delta H_{-1}^\ddagger - \Delta H_2^\ddagger$ change from 4 [L = P(OEt)$_3$] to 33—46 kJ mol^{-1} (L = phosphines). If we assume that to a first approximation the activation enthalpy reflects the electronic requirements, this again indicates a weak Mo–CO bond interaction in (1)‡, and an important Mo–L in (2)‡. It should also be pointed out that these high values are in contrast to those of *ca.* 0 usually expected for ligand recombination in co-ordinatively unsaturated intermediates. In particular, considering that $\Delta H^\ddagger$ must be positive, one can define a low limit of 46 kJ mol^{-1} for $\Delta H_{-1}^\ddagger$, the activation enthalpy for recombination of CO. No specific trend of $\delta\Delta H^\ddagger$ with the electronic character of the phosphorus ligands is observed; however, as expected on the basis of its lower basicity, the $\Delta H_2^\ddagger$ value for attack of P(OEt)$_3$ is higher than those for the phosphines and comparable with that of CO.

The activation entropy differences, $\Delta S_{-1}^\ddagger - \Delta S_2^\ddagger$, range from 23 [L = P(OEt)$_3$] to 199 J K^{-1} mol^{-1} (L = PPh$_3$). This clearly indicates that entropic factors are responsible for the easier CO attack on the intermediate. These can easily be seen as the result of the structural deformations which both the intermediate and the entering ligand must undergo in order to produce metal–ligand interaction in the transition state. On the basis of the above values one can speculate that the intermediate is somewhat less tight than the starting complex, or in other words that its entropy is slightly higher or at least comparable. If this is true, the combination of $\Delta S_1^\ddagger$ and the entropy for free CO in solution (158 J K^{-1} mol^{-1}, standard state 1 mol dm^{-3} in decalin)[*] defines an approximate upper limit of -70 J K^{-1} mol^{-1} for $\Delta S_{-1}^\ddagger$. The $[(OC)_4\overline{Mo(\mu\text{-}PEt_2)_2Mo}(CO)_3]$ intermediate should not appreciably change in entropy on passing to the activated complex (1)‡, in fact a long-range Mo–CO interaction was proposed for (1)‡ in step 1, so that the above entropy variation would mainly reflect the decrease in entropy of CO upon its partial co-ordination to the intermediate to give (1)‡.

These considerations on step -1 cannot simply be extended to step 2. The nature of the activated complex (2)‡ seems to imply very important steric constrictions (or entropy reduction) for both $[(OC)_4\overline{Mo(\mu\text{-}PEt_2)_2Mo}(CO)_3]$ and the phosphorus ligand. However, the important point is that the entropic variations for this bimolecular attack on the co-ordinatively unsaturated intermediate seem to be dominated by the size of the entering ligands. A nice quantitative confirmation of this statement is given by Figure 3, which shows the good linear relation obtained by plotting $\delta\Delta S^\ddagger$ *vs.* Tolman's cone angle for the ligands. It is worth noting that the intercept at $\delta\Delta S^\ddagger = 0$ gives a cone angle of 103°, which is somewhat greater than the approximate value (95°) proposed for the CO ligand.[16] This relation appears to be the first quantitative kinetic demonstration that Tolman's cone angle, determined from static models, is a measure of real (or at least relative) steric hindrance in solution under dynamic conditions. The slope of this plot [= 4.6(0.6) J K^{-1} mol^{-1} degree^{-1}] can be assumed as the kinetic selectivity of the intermediate towards the size of entering ligand.

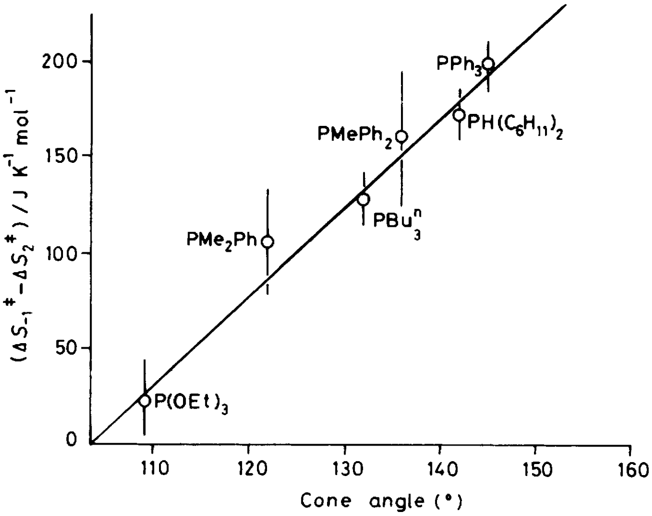

Figure 3. Plot of the activation-entropy differences $\Delta S_{-1}^\ddagger - \Delta S_2^\ddagger$ *versus* phosphorus ligand cone angle for the reaction $[(OC)_4\overline{Mo(\mu\text{-}PEt_2)_2Mo}(CO)_4] + L \rightleftharpoons [(OC)_4\overline{Mo(\mu\text{-}PEt_2)_2Mo}(CO)_3L] + CO$ in decalin. Bars represent approximate standard deviations (see text)

Step -2.—This represents the process with which the monosubstituted complex (2) gives the activated complex (2)‡ in the phosphorus ligand-dissociation reaction. The rate constant for this process, k_{-2}, is in the range (0.8—22) × 10^{-5} s^{-1}, *i.e.* 100—1 000 times lower than for CO dissociation. This is the result of a less favourable activation entropy (12 to -120 J K^{-1} mol^{-1}) not compensated by a lower activation enthalpy (78—133 kJ mol^{-1}). No definite trend in the ligand-dissociation rate with steric or electronic parameters of the leaving group is observed, although, as expected, the rate is slightly lower for the more basic PBu$^n_3$ ligand than with P(OEt)$_3$. Analysis of the obtained activation enthalpy and entropy values shows that both steric and electronic effects are important and that they change in such a way that the k_{-2} value remains almost constant.

It is worth noting the negative activation entropy values, up to -120 J K^{-1} mol^{-1}, which are rather unexpected for a dissociative process. These values do not invalidate the mechanism, but suggest that the same steric requirements that make difficult the approach of the phosphorus ligand, also make difficult its release once the ligand has entered the metal co-ordination sphere. We may envisage that in both cases the ligand must contract (and/or the molybdenum metal centre must open) on crossing the transition state. The same steric effects may also justify the lower activation enthalpy (up to -60 kJ mol^{-1} compared with CO) for the dissociation of the more basic phosphine for which a stronger metal–ligand bond is expected; the release of the steric restrictions on the transition state may represent the 'driving force,' which reduces the enthalpic (or electronic) requirements to metal–phosphorus ligand dissociation.

Acknowledgements

I thank Mr. Antonio Ravazzolo for skilled technical assistance.

---

[*] This value has been calculated from the reported standard entropy of gaseous CO (= 198 J K^{-1} mol^{-1}, standard state 1 atm; National Bureau of Standards, Washington D.C., 1952, Circular 500) by introducing the entropy change (from solubility data in ref. 8) for the solubilisation to the 1 mol dm^{-3} standard state in decalin.

References

1 R. H. B. Mais, P. G. Owston, and D. T. Thompson, *J. Chem. Soc. A*, 1967, 1753.

2 Th. Madach and H. Vahrenkamp, *Chem. Ber.*, 1981, **114**, 513; R. E. Dessy, R. Kornmann, C. Smith, and R. Haytor, *J. Am. Chem. Soc.*, 1968, **90**, 2001 and refs. therein.

3 H. Vahrenkamp, *Chem. Ber.*, 1978, **111**, 3472; M. H. Linck and L. R. Nassimbeni, *Inorg. Nucl. Chem. Lett.*, 1973, **9**, 1105.

4 H. Vahrenkamp, *Angew. Chem., Int. Ed. Engl.*, 1978, **17**, 379; B. F. G. Johnson (ed.), 'Transition Metal Clusters,' Wiley, New York, 1980; M. H. Chrisholm and I. P. Rothwell, *Prog. Inorg. Chem.*, 1982, **29**, 1; D. A. Robert and G. L. Geoffroy, in 'Comprehensive Organometallic Chemistry,' eds. G. Wilkinson, F. G. A. Stone, and E. Abel, Pergamon Press, London, 1982, ch. 40; R. Poilblanc, *Inorg. Chim. Acta*, 1982, **62**, 75; E. L. Meutterties and M. J. Kruse, *Angew. Chem., Int. Ed. Engl.*, 1983, **22**, 135.

5 M. Basato, *J. Chem. Soc., Dalton Trans.*, 1976, 1678.

6 A. J. Carty, *Adv. Chem. Ser.*, 1982, **196**, 163; P. E. Kreter and D. W. Meek, *Inorg. Chem.*, 1983, **22**, 319; R. B. Finke, G. Gaughan, C. Pierpont, and M. E. Cass, *J. Am. Chem. Soc.*, 1981, **103**, 1394; G. Huttner, J. Schneider, H. D. Muller, G. Mohr, J. von Seyerl, and L. Wolfhart, *Angew. Chem., Int. Ed. Engl.*, 1979, **18**, 76; G. L. Geoffroy, S. Rosenberg, P. M. Shulman, and R. R. Whittle, *J. Am. Chem. Soc.*, 1984, **106**, 1519; S-G. Shyu and A. Wojcicki, *Organometallics*, 1984, **3**, 809; R. Regragui, P. H. Dixneuf, N. J. Taylor, and A. J. Carty, *ibid.*, p. 814.

7 E. L. Muetterties, R. R. Burch, and A. M. Stolzenberg, *Annu. Rev. Phys. Chem.*, 1982, **33**, 89.

8 M. Basato, J. P. Fawcett, and A. J. Poe, *J. Chem. Soc., Dalton Trans.*, 1974, 1350.

9 A. A. Frost and R. G. Pearson, 'Kinetics and Mechanism,' 2nd edn., Wiley, Tokyo, 1961, p. 186.

10 M. Basato, *J. Chem. Soc., Dalton Trans.*, 1985, 91.

11 M. Basato and A. J. Poë, *J. Chem. Soc., Dalton Trans.*, 1974, 456.

12 M. Basato, J. P. Fawcett, and A. J. Poë, *J. Chem. Soc., Dalton Trans.*, 1974, 1350.

13 M. Basato, *J. Chem. Soc., Dalton Trans.*, 1975, 911.

14 J. N. Gerlach, S. L. McMullin, and P. C. Ellgen, *Inorg. Chem.*, 1976, **15**, 1232.

15 J. A. C. Howell and P. M. Burkinshaw, *Chem. Rev.*, 1983, **83**, 557; J. D. Atwood, M. J. Wovkulich, and D. C. Sonnenberger, *Acc. Chem. Res.*, 1983, **16**, 350; D. J. Darensbourgh, *Adv. Organomet. Chem.*, 1982, **21**, 113.

16 C. A. Tolman, *Chem. Rev.*, 1977, **77**, 313.

Received 3rd *December* 1984; *Paper* 4/2050